Cylinder-Forming Triblock Terpolymer in Nanopores: A Monte Carlo Simulation Study

Peng Chen[†,‡] and Haojun Liang*[,†,‡]

Hefei National Laboratory for Physical Sciences at Microscale University of Science and Technology of China Hefei, Anhui, 230026, People's Republic of China, and Department of Polymer Science and Engineering University of Science and Technology of China Hefei, Anhui, 230026, People's Republic of China

Received: April 16, 2007; In Final Form: October 26, 2007

This paper systematically investigated the self-assembly of a cylinder-forming $A_{13}B_3C_2$ triblock terpolymer confined in cylindrical nanopores using an annealing Monte Carlo simulation. When the pore wall is absolutely neutral, we observed the helix structures alternating with partial cylinder structures at the outside layer. When the pore wall attracts the shorter blocks, we observed various surface structures depending on the pore wall preference conditions; also, a general inner-layer structural transition sequence was confirmed. In addition, it was found that catenoid structures form in a broad pore diameter region when the pore wall attracts the longest block. This may be used to experimentally fabricate the long-range ordered nanostructure. The differences between this triblock terpolymer system and the cylinder-forming diblock copolymer system were compared, and it was found that the triblock system is more capable of retaining ordered structures under unfavorable confinement conditions.

1. Introduction

Block polymers, a class of macromolecules comprised of two or more chemically distinct polymer blocks, have been intensively studied to determine their ability to self-assemble into various ordered structures on the length scale of 10∼100 nm.[1−3] The confinement effect imposed by bounding surfaces has been applied to control the orientation of the microdomain structures and to produce unusual nanostructures.[4−16]

The self-assembly of compositionally asymmetric systems under confinement, particularly of cylinder-forming block polymers in the bulk, has attracted attention both in the experimental and theoretical fields.[17−26] These studies revealed that the surface preference and frustration between the confinement dimensions and the polymers' bulk equilibrium period induce the orientation of a cylindrical structure and the formation of noncylindrical structures. To study the simple confinement case, which is under planar confinement, Knoll et al. experimentally studied the phase diagram for a cylinder-forming ABA triblock copolymer system in a film corroborated by a dynamic density functional theory (DDFT) simulation.[19] Some deviations from the bulk cylinder structure, such as perforated lamella and wetting layer, were observed in their study and were believed to be dominated by surface reconstructions. When the confinement geometry was a two-dimensional cylindrical nanopore, it was found that the cylinder system could adopt a coiling strategy to form helixes and doughnuts in the confinement pore.[21] Yu et al. carried out a systematic Monte Carlo study of the confinement-induced formation of the unusual structures in the confined cylinder-forming diblock copolymer system.[26] As they asserted, the origin of these novel structures is the confinement-induced structural frustration, which has been substantiated by the subsequent self-consistent field theory (SCFT) study.[27]

Most of the previous studies focused solely on two-component systems, such as AB diblock or ABA triblock copolymers. Meanwhile, there are relatively fewer studies on the more complex block polymer system, such as the cylinder-forming ABC triblock terpolymer. Ludwigs and co-workers once reported a highly ordered hexagonally perforated lamella structure on the basis of a cylinder-forming ABC triblock terpolymer thin film. In addition, they also investigated film morphology as a function of film thickness.[20,28,29] As a theoretical study, we carried out a systematic Monte Carlo simulation on the self-assembly of a cylinder-forming ABC triblock terpolymer in thin films.[23] We found that although the cylinder structure formed by a triblock terpolymer appeared similar to that formed by a diblock copolymer, the additional middle block in the triblock terpolymer system makes them form different structures and experience different structure transitions under confinement conditions. Very recently, Feng and Ruckenstein reported a Monte Carlo research on the self-assembly of ABC linear triblock copolymers in a nanocylindrical tube.[30] They concentrated on three kinds of chain architectures ($A_5B_5C_5$, $A_5B_{10}C_5$, and $A_5B_5C_{10}$) and studied the effect of tube diameter and tube surface preferences for different segments on self-assembled morphologies. A variety of helixes and plate and dendrite structures were found in their study.

In this work, we performed the annealing Monte Carlo study on the cylinder-forming ABC triblock terpolymer system confined in cylindrical confinement conditions. Here, the ABC triblock terpolymer readily forms hexagonally arranged cylinder structures in the bulk, and we studied the self-assembly of this cylinder-forming ABC triblock terpolymer in nanopores, considering different pore wall surface preferences and pore diameters. Because previous studies on cylinder-forming diblock copolymers self-assembly under cylindrical confinement showed that the formation of confinement-induced structures is correlated with the ratio between the pore diameter D and the cylinders' spacing in the bulk L (that is, D/L),[26] we observed the structural transition along with the values of D/L. To study

* To whom all correspondences should be addressed: hjliang@ustc.edu.cn.
† Hefei National Laboratory for Physical Sciences at Microscale University of Science and Technology of China Hefei.
‡ Department of Polymer Science and Engineering University of Science and Technology of China Hefei.

10.1021/jp072942x CCC: $40.75
Published on Web 01/25/2008

the surface structures of the triblock terpolymer system, we calculated the ensemble-average surface chain orientation values and component fractions when the pore wall is neutral to any block. We observed a variety of self-assembled structures that are different from previous studies. We also found that the triblock terpolymer exhibits a good ability to retain a regular structure under confinement conditions, and as a result, it might be more suitable for fabricating long-range ordered nanostructures than the diblock copolymer system. We therefore believe our exploration would provide some useful information for subsequent experimental studies.

2. Model

2.1. Annealing Monte Carlo Simulation. Similar to our previous study, we performed annealing Monte Carlo simulations in a canonical ensemble in the framework of a simple cubic lattice model.[23]

In the move set, we used the vacancy diffusion algorithm combined with the single-site bond fluctuation model (i.e., the bond is 1 or $\sqrt{2}$ in the unit of lattice size). The evolution of chain configuration is realized by randomly displacing a vacancy to a monomer in its 18 neighboring sites only if there is no bond crossing. The Metropolis Rule is used to govern each step of the movement. A movement try is accepted if the energy change is less than zero; otherwise, it is accepted with a probability $P = \exp(-\Delta E/kT)$, where ΔE is the energy change of the movement, k is the Boltzmann constant (is set to 1), and T is the system temperature. The value of ΔE can be expressed as

$$\Delta E = (\Delta N_{AB}\epsilon_{AB} + \Delta N_{AC}\epsilon_{AC} + \Delta N_{BC}\epsilon_{BC} + \Delta N_{SA}\epsilon_{SA} + \Delta N_{SB}\epsilon_{SB} + \Delta N_{SC}\epsilon_{SC})$$

where ΔN is the difference between the number of pairs of neighboring sites occupied by monomers A, B, C, and the surface site S; and ϵ is the repulsion interaction between different segments or the segment with surface site. One Monte Carlo step (MCS) means all monomers in the system tried one movement.

On the basis of the above canonical ensemble Monte Carlo simulation, we employed an annealing strategy to gradually quench the system from the initial homogeneous state to the production state. This annealing strategy has been powerfully demonstrated in Monte Carlo studies on phase separation.[15,23,26,31−33]

A schedule of $T_{j+1} = fT_j$ is set in the stepwise annealing process, where T_j is the relaxation temperature at the jth annealing step, and f is the scaling factor. The annealing procedure implies that a homogeneous system runs from the initial temperature T_0 and reaches the equilibrium temperature T_f after predetermined N annealing steps. During each annealing step, the relaxation temperature is constant. In this study, the temperature began at $T_0 = 10.0$ and reached $T_f = 1.85$ after 17 steps ($f = 0.9$). During each annealing step, we performed at least 400 000 Monte Carlo steps (MCS).

2.2. System Parameters. In this study, the monomer volume fraction was set at 70% (that is, 70% of all lattice sites were occupied by monomers) both in the bulk and in the confinement cases to reproduce a melt behavior in our simulations. Although on one occasion we tried different monomer volume fractions in the simulation (such as 60% and 90%, etc.), the self-assembly seemed less affected with different monomer volume fractions. To get the chains evenly dispersed and to ensure the same volume fraction in the bulk box and the pore confinement conditions, we selected the 70% fraction rate for all tests undertaken for this paper. In the bulk, we imposed the periodic boundary conditions (PBCs) in all directions. Meanwhile, in the confinement cases, PBCs were only imposed in the z direction, which was the long axis in the cylindrical nanopore confinement. The pore length was either 54 or 60 in lattice size to ensure that the structures were stable and to obtain the optimum regular structure in the simulations. We set a circular boundary with a diameter of D for the x and y directions in the confinement cases.

As limited by our computers' calculation capability, we chose the total chain length in this study as 18. That is very short in comparison with true polymer chains, but the phase separation in simulation seems to be less affected by the block length, considering that the monomer is a coarse-grained model in the simulation. The triblock terpolymer was simulated with the chain architecture $A_{13}B_3C_2$. A, B, and C represented three types of monomers, and the repulsions between these monomers were all set at 1.0, that is, $\epsilon_{AC} = 1.0$, $\epsilon_{AB} = 1.0$, and $\epsilon_{BC} = 1.0$. This means that these three types of monomers strongly repel one another. In such polymer chain parameter settings, the system forms hexagonally arranged cylinder structures in the bulk. In the confinement conditions, we considered six kinds of pore wall preference cases, which are (1) neutral wall, wherein the pore wall is neutral to all blocks, that is, $\epsilon_{SA} = 0$, $\epsilon_{SB} = 0$, and $\epsilon_{SC} = 0$; (2) A-attractive wall, the pore wall only attracts A-blocks, that is, $\epsilon_{SA} = -1.0$, $\epsilon_{SB} = 0$, and $\epsilon_{SC} = 0$; (3) B-attractive wall, the pore wall only attracts B-blocks, that is, $\epsilon_{SA} = 0$, $\epsilon_{SB} = -1.0$, and $\epsilon_{SC} = 0$; (4) C-attractive wall, the pore wall only attracts C-blocks, that is, $\epsilon_{SA} = 0$, $\epsilon_{SB} = 0$, and $\epsilon_{SC} = -1.0$; (5) B/C-attractive wall, wherein the pore wall attracts both B-blocks and C-blocks simultaneously, $\epsilon_{SA} = 0$, $\epsilon_{SB} = -1.0$, and $\epsilon_{SC} = -1.0$; and (6) A/C-attractive wall, wherein the pore wall attracts both A-blocks and C-blocks, $\epsilon_{SA} = -1.0$, $\epsilon_{SB} = 0$, and $\epsilon_{SC} = -1.0$.

2.3. Chain Orientation Value and Components Fraction Values. As the triblock terpolymer system was confined in a cylindrical nanopore, the surface chains that touched the pore wall experienced special frustration. To study the chain configuration at the surface, we calculated the ensemble-average chain orientation values and components fraction values for the chains if one or more of their 18 monomers resided at the surface. After the system temperature reached $T_f = 1.85$ and the equilibrium structure was formed, we collected 1000 successive configurations with the interval of 5 MCS. This is similar to the procedure in the study of Wang et al., which we also previously performed.[18,23] The ensemble-average values were calculated from these configurations. For the components fraction value, we refer to it as the percentage of one component distribution versus all three components' distribution at the surface.

For the chain orientation value, we defined a chain orientation vector from the A-block's center of mass to that of the C-block, and the orientation angle θ is defined as the angle between this chain orientation vector and the pore long axis direction (z-direction). We calculated the ensemble-average absolute value of cos θ (i.e., $\langle|\cos\theta|\rangle$) to represent the chain orientation, and the criterion $\langle|\cos\theta|\rangle = (1/\pi)\int_0^{\pi}|\cos\theta|\mathrm{d}\theta = 2/\pi$[18,23] was applied to judge the chains orientation, that is, whether they are parallel or perpendicular to the pore long axis (z) direction. As we know, the chains were mainly perpendicular to the pore surface (that is, the chains were mainly perpendicular to the pore long axis) if $\theta \approx \pi/2$, thus $\langle|\cos\theta|\rangle < 2/\pi$. In contrast, they were mainly parallel to the pore surface if $\theta \approx 0$ or π, thus $\langle|\cos\theta|\rangle > 2/\pi$.

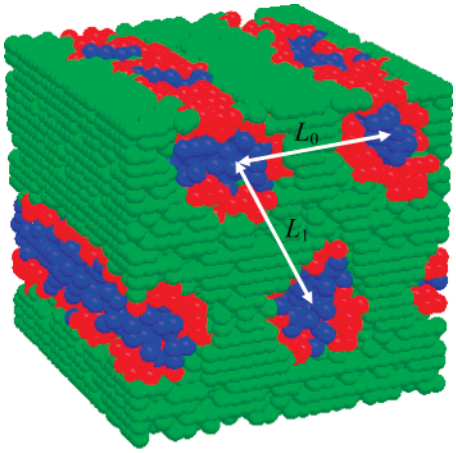

Figure 1. Cylinder structure of triblock terpolymer $A_{13}B_3C_2$ in the bulk: blue, C-blocks; red, B-blocks; green, A-blocks. The colors shown are all the same in the following figures. L_0 and L_1 refer to the neighboring cylinder spacing.

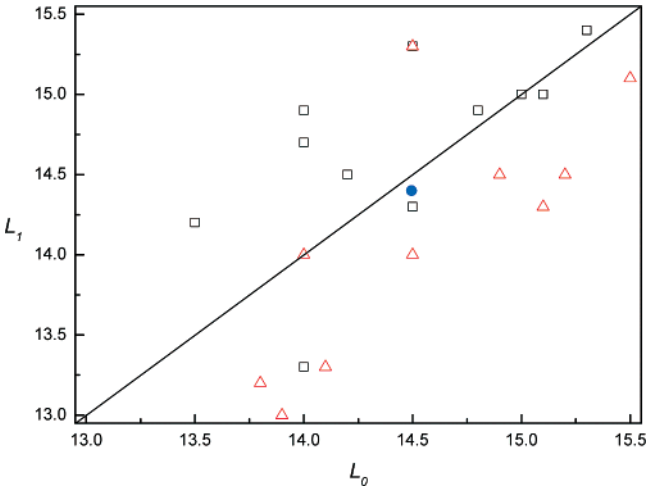

Figure 2. Bulk simulation results of triblock terpolymer $A_{13}B_3C_2$ in different runs. L_0 and L_1 are cylinder spacing shown in Figure 1. For box dimension $Lx \times Ly \times Lz$, □ represents $26 \times 27 \times 28$, △ represents $25 \times 28 \times 30$, and ● represents the average values of L_0 and L_1.

3. Results and Discussion

3.1. In the Bulk. Figure 1 shows that the self-assembled structure of the triblock terpolymer $A_{13}B_3C_2$ in the bulk was hexagonally arranged core−shell cylinders. In these cylinders, the C-blocks formed a core, the B-blocks formed the shell covering the C-blocks' core, and the majority component A-blocks formed the matrix. To calculate the cylinders' period L in the bulk, we performed bulk simulation with different system box dimensions. On the basis of our computations, we found that two boxes with the dimensions $Lx \times Ly \times Lz$: $26 \times 27 \times 28$ and $25 \times 28 \times 30$ (all in lattice size) were apt to form the hexagonally arranged cylinder structures, which were parallel to the box surfaces. This means that the box dimensions are commensurate with the cylinders' period. We defined the distance between the two nearest cylinders parallel to the box surface as L_0 and the distance of the other nearest cylinders as L_1, as shown in Figure 1. To ensure that the cylinders had a hexagonal arrangement, we limited the condition $|L_0 - L_1| < 1$. The cylinder periods at different runs are presented in Figure 2. We got the average values of $L_0 = 14.5$ and $L_1 = 14.4$ (both in lattice size). Thus, the cylinder period L in this study was about 14.5 in lattice size.

In the following studies, we changed the pore diameter D under different pore wall surface preferences. The confinement dimension was represented as D/L. All self-assembled structures under different conditions are summarized in Table 1. We shortened the structures' names as follows: C, cylinder; *f*C, flat cylinder; B, bar-shaped; H, helix; *d*H, double helix; W, irregular wetting layer; *s*W, striplike wetting layer; T, toroid; and D, droplet. We combined these structures together to name a complex structure. For example, "6B(*f*C)" means it has an outer-layer six bars and an inner-layer flat cylinder structure. Although we distinguish the helix "H", bars "B", flat cylinders "*f*C", and cylinders "C" (those could be seen as a set of deformed cylinder or partial cylinder structures) only by visual inspection and we have no thermodynamic data to suggest that these structures are thermodynamically distinct phases, such structures are unvaried when changing pore lengths and in different simulation runs. This made us believe such cylinder deformations are energy-favored for the block polymers self-assembly under the pore confinement.

3.2. Under Neutral Wall. At first, we considered the self-assembled structures when the pore wall had no preference for any block. In the scope of our study, the triblock system began with a one-layer double-helix structure (*d*H) at $D/L = 1.03$ and ended with a two-layer double-helix structure (*d*H(*d*H)) at $D/L = 3.1$. In Table 1, we can see the bar-shaped structures alternated with the helix structures as D/L increased. It seemed that in the neutral wall case, the structural transition with D/L increasing for the triblock terpolymer system was very similar with that for the diblock copolymer system. Yu et al.[26] discovered that for the diblock copolymer A_3B_9 at $D/L \approx 1.1$, it was a double-helical structure, and at $D/L \approx 1.2$ or 1.3, it was a three-cylinder structure (as in Figure 1c of ref 51). This corresponds well with our double helix (*d*H at $D/L = 1.03$) and three-bar structure (3B at $D/L = 1.17$ and 1.31). For $D/L > 1.3$, the diblock copolymers experienced a phase region for helical or toroid structures ($D/L \approx 1.5$), then entered a parallel cylinder region ($D/L \approx 2.0$), and then entered another helix region ($D/L \approx 3.0$). The similar structural transition tendency, which is from helix to parallel cylinders and then to helix again, was also observed in Table 1 neutral wall cases. For the triblock terpolymer $A_{13}B_3C_2$ system, we also found that (a) when the pore diameter is small ($D/L < 2.55$), the bars are more robust than the helix at the outer layer; moreover, when the pore diameter is in the scope of $2.55 < D/L < 3.1$, there are all helix structures; (b) the inner-layer structures grow from a cylinder ($D/L = 1.72 \sim 2.14$) to a flat cylinder ($D/L = 2.28 \sim 2.41$) and then to a helix ($D/L = 2.55 \sim 3.1$). It seems that this inner-layer structural transition is due to the increase in minority block (BC) materials as the pore diameter increases. That is, when the materials are more than what a regular cylinder structure would consume, there forms a flat cylinder structure which could consume more material while retaining a regular structure. Furthermore, when there is more material in larger pores, then helix structures are formed to make use of all these materials.

In Figure 3, it appears that the system created partial cylinders adjacent to the pore wall, that is, the cylinder cores at the pore wall are those partially surrounded by the corona (the B-block shell and A-block matrix). This means all three components are in contact with the pore surface. Such partial cylinders might form bars or helix structures. The bars (all in the outer layer) and outer-layer helix structures were striplike geometries with narrow cross sections adjacent to the surface. Correspondingly, the inner-layer structures were cylinder-like, being cylinders and flat cylinders, or twist-cylinder-like (helix) geometries. Although

TABLE 1: Self-Assembled Structures as a Function of the Ratio of Pore Diameter *D* versus Polymer Period *L*, *D*/*L*, with Different Pore Wall Surface Preferences[a]

	pore wall surface preference					
D/*L*	neutral	A-attractive	B-attractive	C-attractive	B/C-attractive	A/C-attractive
1.03	*d*H	C	W	*s*W	W	3B
1.17	3B	*f*C	W	*s*W	W	3B
1.31	3B	*f*C	W	*s*W	W	4B
1.45	*d*H	peapod	W(D)	*s*W(D)	W(D)	4B
1.59	4B	peapod	W(C)	*s*W(D)	W(C)	4B(D)
1.72	4B(C)	catenoid	W(C)	*s*W(D)	W(C)	4B(C)
1.86	3H(C)	catenoid	W(C)	*s*W(C)	W(C)	6B(C)
2.00	5B(C)	catenoid	W(C)	*s*W(C)	W(C)	6B(C)
2.14	5B(C)	catenoid	W(C)	*s*W(C)	W(C)	6B(C)
2.28	5H(*f*C)/6B(*f*C)	catenoid	W(*f*C)	*s*W(C)	W(*f*C)	6B(*f*C)
2.41	6B(*f*C)	catenoid	W(*f*C)	*s*W(*f*C)	W(*f*C)	6B(*f*C)
2.55	*d*H(*d*H)	catenoid	W(H)	*s*W(*f*C)	W(H)	6B(*f*C)
2.69	*d*H(*d*H)	catenoid(C)	W(H)	*s*W(*d*H)	W(H)	*s*W(*d*H)
2.83	*d*H(*d*H)	catenoid(C)	W(H)	*s*W(*d*H)	W(T)	*s*W(*d*H)
2.97	H(H)	catenoid(C)	W(H)	*s*W(H)	W(*d*H)	*s*W(*d*H)
3.10	*d*H(*d*H)	catenoid(C)	W(T)	*s*W(H)	W(*d*H)	H(H)

[a] B, bar-shaped; H, helix; *d*H, double-helix; C, cylinder; *f*C, flat cylinder; peapod, peapodlike cylinder; catenoid, cylindrical catenoid sheet; W, irregular wetting layer; D, droplets; T, toroid; *s*W, striplike wetting layer. The number before B and H means the number of corresponding structure at the same layer.

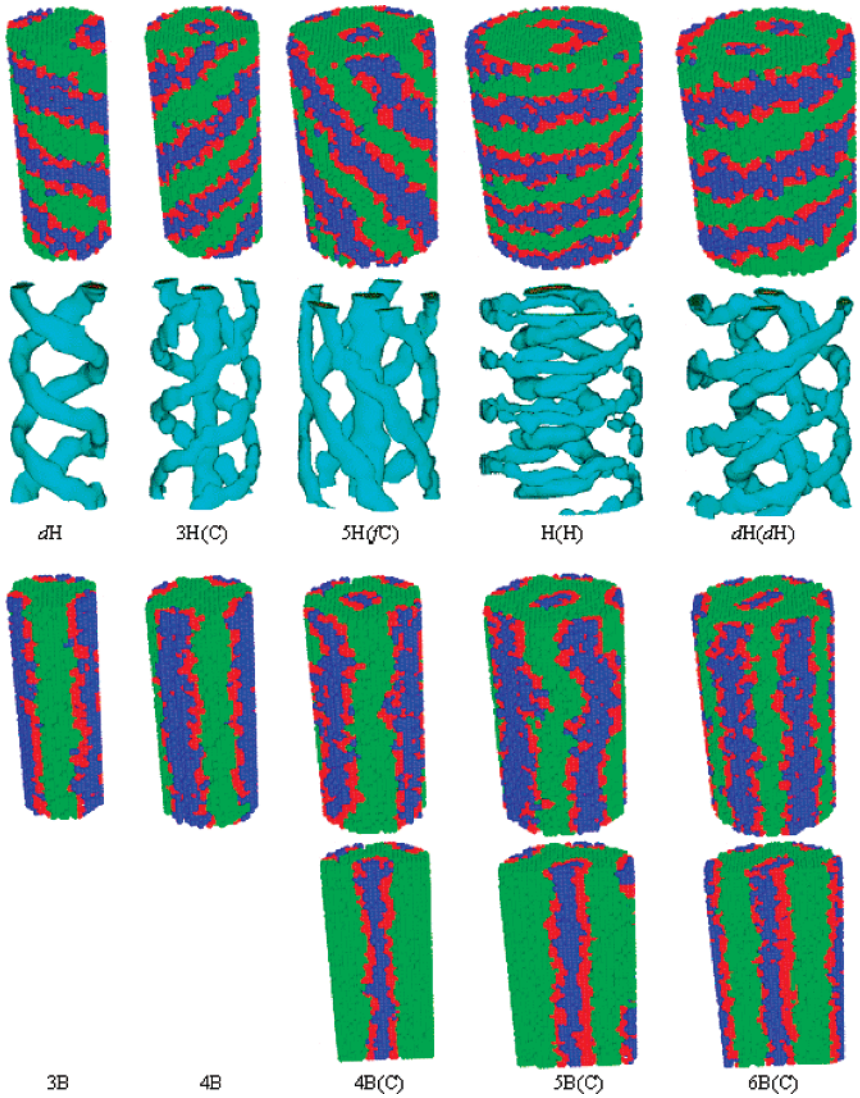

Figure 3. Typical self-assembled structures of triblock terpolymer $A_{13}B_3C_2$ under neutral pore wall condition. The structures correspond to the signs summarized in Table 1, and in some cases, C-block isodensity surfaces (the second line) of inner-layer structures or cross sections (the fourth line) of some structures are shown for clarity.

both the cylinder-like structures (cylinders, flat cylinders, and inner-layer helix) and striplike structures (bars and outer-layer helix) can be taken as the transformation of regular cylinder structures, the cylinder-like structures have broad cross sections

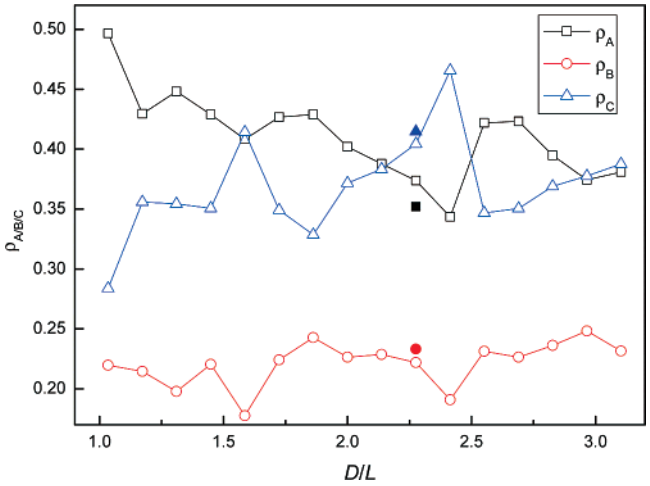

Figure 4. Ensemble-average component fraction distributions at the surface $\rho_{A/B/C}$ of the self-assembled structures under neutral wall condition as a function of D/L. ρ_A, ρ_B, and ρ_C represent corresponding fraction of A-block, B-block, and C-block, respectively. The filled signs represent those for the degenerate structure 6B(*f*C) at $D/L = 2.28$.

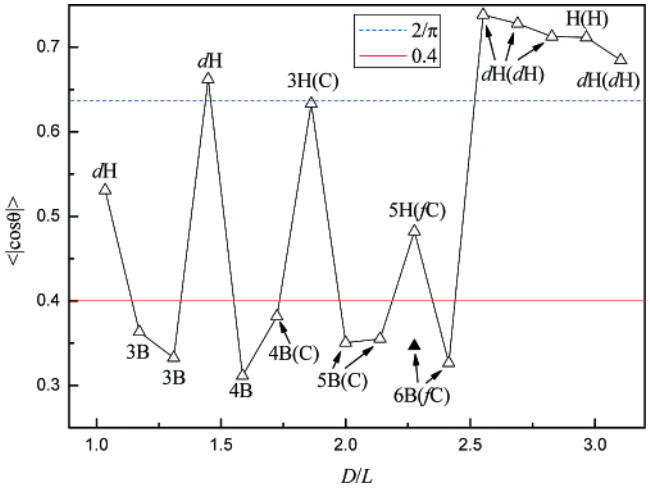

Figure 5. Ensemble-average surface chain orientation values $\langle|\cos\theta|\rangle$ of the self-assembled structures under neutral wall condition as a function of D/L. The filled symbol ▲ represents that for the degenerate structure 6B(*f*C) at $D/L = 2.28$.

in comparison with those of the striplike ones. This probably comes from the fact that the chains at the surface suffered from a more severe extension or compression than those from the inner-layer structures.

The components fraction values (Figure 4) show that in most cases, the C-block and B-block fraction values at the surface are higher than those in the bulk, which are 0.11 (C-blocks: 2/18) and 0.17 (B-blocks: 3/18), respectively. We also found that the C-block fraction value at the surface experienced two relative increases ($D/L = 1.59$ and 2.41 in Figure 4), while the B-block and A-block fraction values dropped simultaneously. Such undulations happened when the pore diameter D was incommensurate with the polymer period L ($D/L \approx 1.5$ and 2.5, that are half of integers), which are also the structural transition points. We conjecture that the undulations might originate from a structure frustration-induced polymer chain adjustment.

Being different from diblock copolymer system under the same pore confinement condition, the triblock terpolymer system shows an excellent capability to keep a well-ordered structure. In most cases, when we repeat the simulations from different random initial states or change the pore length, the self-assembled structures are less affected, except for that in $D/L = 2.28$ with neutral surface where two degenerate structures form. In contrast to this, in the diblock copolymer system, Yu et al. observed some degenerate structures at the same confinement dimension with neutral pore wall (as in Figure 1c of ref 51).

We observed that for all bar structures, the surface chain orientation values were far less than $2/\pi$, as we show in Figure 5. Using a line, they are all less than a constant of 0.4 (we used such a constant only for the convenience of visual judgment), which means that the chains are mainly perpendicular to the pore wall. For most of the helix structures, the surface chain orientation values are beyond or about the criterion line ($2/\pi$). This means that the chains are mainly parallel to the pore wall, except for the helix structures at $D/L = 1.03$ and 2.28, which are less than the criterion line ($2/\pi$) but are beyond the line of 0.4. At $D/L = 1.03$, the pore diameter ($D/L \approx 1.0$) was apt for the chain stretching at the perpendicular direction, which could induce the chain stretching orientation. At $D/L = 2.28$, as Table 1 shows, the helix structure 5H(*f*C) was a degenerate in relation to the bars structure (6B(*f*C)). Figure 3 shows that the helix pitch of 5H(*f*C) was far larger than those of other helix structures. Therefore, we conjecture that the 5H(*f*C) was a dubious metastable structure which could be an outer-layer distorted bar and an inner-layer flat cylinder structure, such as 5B(*f*C). Such a metastable structure could easily be ruled out by comparing free energy in self-consistent field theory (SCFT) calculation, and we can only report it here as a degenerate structure because of lacking free-energy data in our Monte Carlo simulation. For this degenerate structure, the bar structure 6B(*f*C) at $D/L = 2.28$ $\langle|\cos\theta|\rangle \approx 0.346$, the chains were mainly perpendicular to the pore wall.

3.3. Under the A-Attractive Wall. It was observed in studies on diblock copolymer self-assembly within cylindrical nanopores that the pore wall preference for longer or shorter blocks acts similarly on the system's structural transition because of the screening effect of the first layer to the pore wall. However, for the triblock terpolymer $A_{13}B_3C_2$ system, the structural transitions were far different for those in the A-attractive wall case than for those in the B- or C-attractive wall case. In the A-attractive wall case, the wall was totally occupied by A-blocks, while the C- and B-blocks were repelled into the pore center. At the same time, a good "ABC" order for chain stretching from the surface was retained.

When the confinement dimension $D/L \leq 1.59$, as shown in Table 1, the structures developed from a cylinder (C at $D/L = 1.03$) to flat cylinders (*f*C at $D/L = 1.17$ and 1.31) and then to peapodlike cylinders (peapod at $D/L = 1.45$ and 1.59). Figure 6 shows that for these peapodlike cylinders, the inner-layer A-blocks gathered into droplets in the cylinder-like structure of the B- and C-blocks. When the confinement dimension $D/L \geq 1.72$, the system transformed into catenoid structures. The catenoid structure was a B−C−B block cylindrical sheet perforated by the A-block domain, which was identical with the perforated lamella structure within the thin film in a block arrangement,[20] and a coiling strategy[21] was adopted under cylindrical confinement. The perforation density increased as the pore diameter increased, and the inner cylindrical structure was formed when there was enough material ($D/L = 2.69\sim3.1$). In a recent study, Feng and Ruckenstein observed the perforated curved lamella for triblock system self-assembly in nanocylindrical tubes.[30] The perforation of the curved lamella occurs at the surface, which is different from the catenoid structure in this study, in which the perforation occurs far from the surface. Such a catenoid structure exists in a very large pore diameter region that is from $D/L = 1.72$ to 3.10 in this study. There are no large pore diameter regions for one regular structure in the

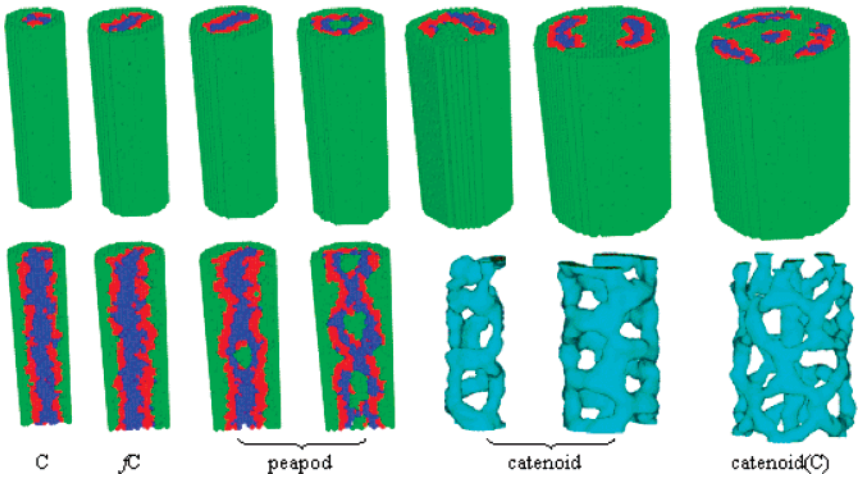

Figure 6. Typical self-assembled structures of triblock terpolymer $A_{13}B_3C_2$ under A-attractive wall condition. The cross sections of the first four structures and the inner-layer C-block isodensity surfaces of the last three ones are shown under the corresponding structures.

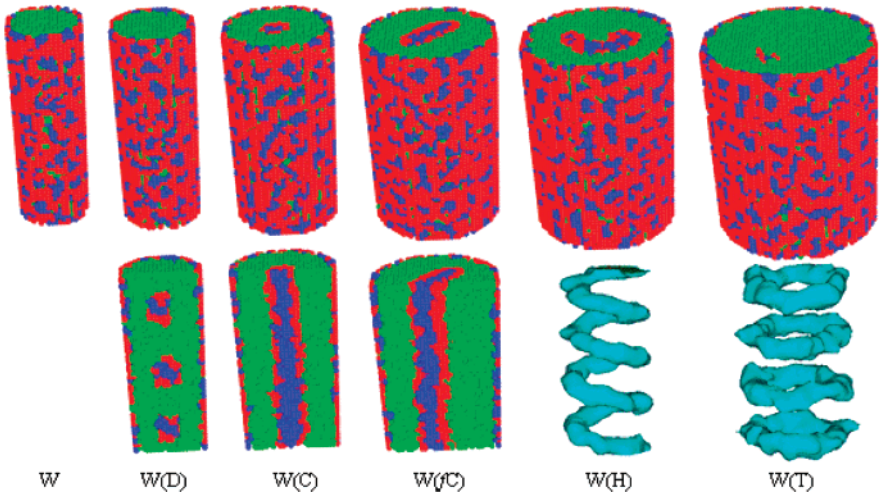

Figure 7. Typical self-assembled structures of triblock terpolymer $A_{13}B_3C_2$ under B-attractive wall condition. The cross sections of some structures and the inner-layer C-block isodensity surfaces of the last two ones are shown under the corresponding structures.

studies on diblock copolymer systems by Yu et al. and Li and Wickham.[26,27]

In experiments, it is difficult to fabricate long-range ordered structures partly because of the undulation of film thickness or pore diameter. It has been demonstrated that the different film thickness and pore diameter values favored different structures in most cases. Since the catenoid structure in the $A_{13}B_3C_2$ system was equilibrated in a large range of pore diameters, we expected that the experiment could easily observe the well-developed long-range order. Ludwigs et al. fabricated this catenoid structure (hexagonally perforated lamella)[20] in a large film with a scale of $12 \times 4\ \mu m^2$. This can also be realized under a cylindrical nanopore confinement.

3.4. Under the B-Attractive Wall. When the pore wall attracted the B-block, the middle block of the ABC triblock chain, the wall drew the B-block together with the C-block adjacent to the surface because of the architecture connection, as we demonstrated in a previous triblock terpolymer study.[23] Therefore, the outer layer of the self-assembled structures under the B-attractive wall was a mixture of B-block and C-block wetting layer ("W" in Table 1, B-attractive case). Such a wetting layer had no regular pattern, and it screened inner-layer structures from the wall surface effect. As a result, the inner structures rose from a line of droplets (D) to cylinders (C) as the pore diameters increased and then to flat cylinders (*f*C) when the materials assumed a more than regular circular−cylindrical structure. Finally, the system formed helix (H) and toroid (T) structures. These are shown in Figure 7.

3.5. Under the C-Attractive Wall. A similar structure transition sequence under the B-attractive wall, from droplets (D) to cylinder (C) and flat cylinder (*f*C) and then to helix (*d*H or H), was also found under C-attractive wall conditions as Table 1 C-attractive shows. The difference between the B-attractive wall case and the C-attractive wall case was the outer-layer structure. For the C-attractive wall case shown in Figure 8, the C-blocks preferentially wet the wall surface to form a striplike outer-layer structure. As a result, the B-blocks were repelled from the surface, and the system formed a CBA order from the surface in components sequence.

3.6. Under the B/C-Attractive Wall. Table 1 shows that when the pore wall showed a preference for both of the shorter blocks, B- and C-block, the triblock terpolymer $A_{13}B_3C_2$ system exhibited the same structure transition sequence of inner-layer structures as that in the B-attractive and C-attractive cases. Moreover, the outer-layer structures under the B/C-attractive wall were the irregular wetting layer, similar to the B-attractive wall but with more C-blocks (Figure 9).

Under the conditions wherein the pore wall has preference for short blocks (B-attractive, C-attractive, and B/C-attractive cases), the outer-layer structures were always irregular. On the other hand, the inner-layer structure transition sequence for the triblock terpolymer $A_{13}B_3C_2$ system was similar to the one for

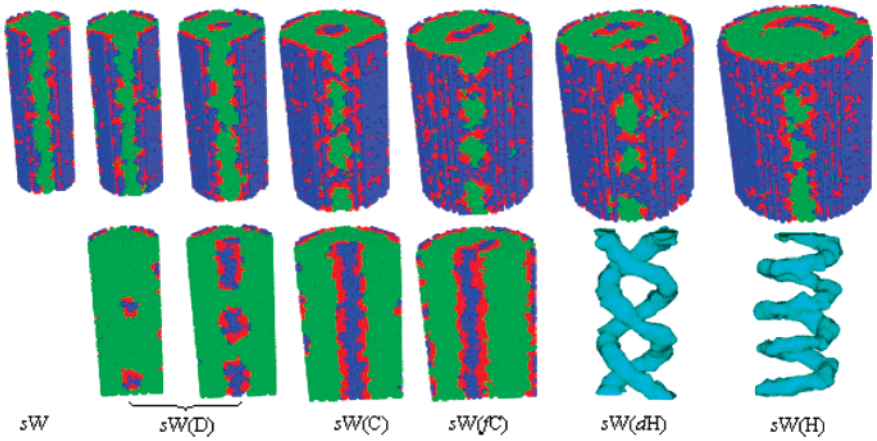

Figure 8. Typical self-assembled structures of triblock terpolymer $A_{13}B_3C_2$ under C-attractive wall condition. The cross sections of some structures and the inner-layer C-block isodensity surfaces of the last two ones are shown under the corresponding structures.

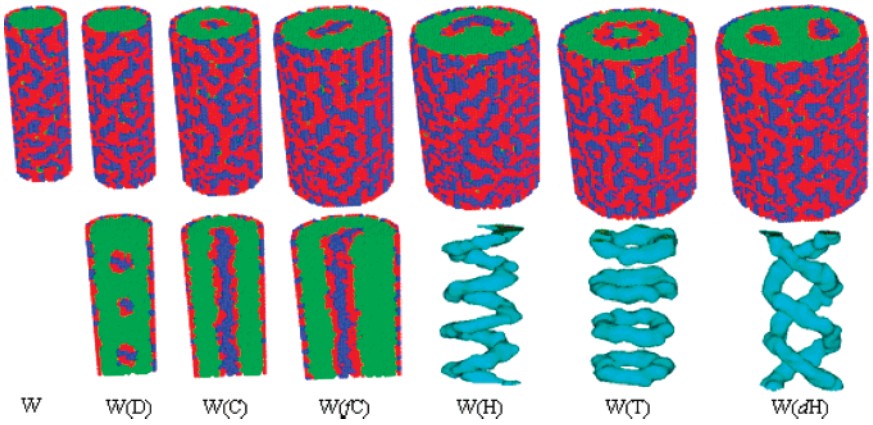

Figure 9. Typical self-assembled structures of triblock terpolymer $A_{13}B_3C_2$ under B/C-attractive wall condition. The cross sections of some structures and the inner-layer C-block isodensity surfaces of the last three ones are shown under the corresponding structures.

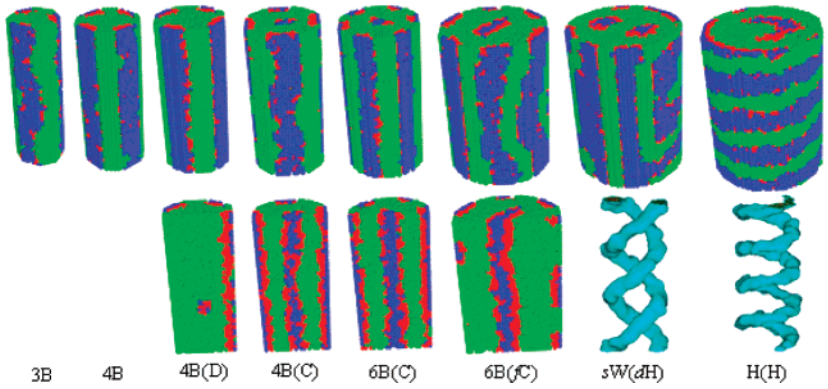

Figure 10. Typical self-assembled structures of triblock terpolymer $A_{13}B_3C_2$ under A/C-attractive wall condition. The cross sections of some structures and the inner-layer C-block isodensity surfaces of the last two ones are shown under the corresponding structures.

the cylinder-forming diblock copolymer system. However, the same structures in the triblock system occurred at smaller confinement dimensions (D/L) than those in the diblock system. Examples of these for the triblock system are the inner-layer cylinder structures under the conditions where the wall attracts shorter blocks, which appeared at the range of $1.59 \leq D/L \leq 2.28$, while for the diblock system A_2B_{10}, the inner-layer cylinder appeared at $2.3 \leq D/L \leq 2.7$.[26]

3.7. Under the A/C-Attractive Wall. Because the self-assembled structures were markedly different at the A-attractive wall case compared with those at the C-attractive wall case, we considered the fact that the pore wall attracted both A-block and C-block. As Table 1 and Figure 10 show, the inner-layer structural transition was similar to that in the C-attractive wall case, that is, the transition was from the dispersed droplets to cylinder to flat cylinder and then to helix as the pore diameter increased. However, the outer-layer structures were quite different from those in the A-attractive or the C-attractive wall cases. Although the C-blocks were preferentially attracted on the surface similar to the C-attractive wall case, the A-blocks were also attracted on the surface. This pushed the gathering outer-layer C-blocks into the bar structure (B in Table 1, A/C-attractive case). The difference between these bar structures from those in the neutral wall case was that the B-blocks were more strictly repelled from the surface in the A/C-attractive case. At the outer layer, when $D/L \leq 2.55$, the number of bars increased gradually from 3 to 4 and then to 6. After experiencing a region of irregular striplike wetting layer structures (*s*W in Figure 10),

the outer layer formed a helix structure at $D/L = 3.1$. Given this, at $D/L = 3.1$, the triblock system formed a very special H(H) structure which was similar with the H(H) structure formed during the neutral wall case, with the B-blocks more strictly repelled from the surface in the A/C-attractive case.

3.8. Comparison with Other Simulation Work. When we finished this work, Feng and Ruckenstein published their Monte Carlo study on linear ABC triblock copolymers self-assembly in nanocylindrical tubes.[30] As they did not reveal what their triblock copolymers self-assemble into in the bulk, we conjecture that their systems might form lamellae or gyroid structures in the bulk partly because of the perpendicular lamellae (such as S1 in Figure 1 of ref 30) and the parallel lamellae (such as S27 in Figure 1 of ref 30) structures formed in their study.

Although the $A_5B_5C_{10}$ system in Feng and Ruckenstein's study is highly asymmetric in chain architecture and just resembles our $A_{13}B_3C_2$ system, which might form cylinder structures in the bulk, we found a difference between the typical structures of their study and our study. For example, the helix structures in their study are in pairs (such as S4, S5, and S22), which is different from the helix structures in our $A_{13}B_3C_2$ cylinder-forming system and which have no counterparts. In addition, the perforated curved lamella such as S8 and S25 in Feng and Ruckenstein's study is similar to the catenoid−cylinder structure in our study on a lamellae-forming symmetric diblock copolymer,[12] that is, the perforation occurs adjacent to the surface. This is also different to the catenoid structure in this cylinder-forming $A_{13}B_3C_2$ triblock terpolymer system, in which the perforation occurs far from the surface. Therefore, we think that the study by Feng and Ruckenstein discovered a variety of novel structures self-assembled by lamellae or gyroid-forming triblock terpolymers. In contrast, our study concentrated on the cylinder-forming triblock terpolymer system.

4. Conclusions

With the annealing Monte Carlo study on cylinder-forming triblock terpolymer $A_{13}B_3C_2$ self-assembly under a cylindrical nanopore, we found the general inner-layer structural transition sequence, that is, from droplets to cylinder to flat cylinder and then to helix, except in the A-attractive wall case. Such a structural transition sequence was similar to the one in the diblock copolymer system under cylindrical nanopore confinement. However, we did not observe the effect of the D/L value (integer or half an integer) on the structural orientation in this triblock terpolymer $A_{13}B_3C_2$ system, and the increasing of material seemed to be the dominant force pushing the structural transition. The outer-layer structures depended strongly on the preference of the surface. In the neutral wall case, the bar structures altered with the helix structures at the outer layer. In cases where the wall attracts shorter blocks, the outer-layer structures were irregular wetting layers. In the A/C-attractive wall case, the outer layer could be bars or striplike wetting layers.

When the pore wall attracted the majority block, the A-block in this $A_{13}B_3C_2$ system, there was no structure at the surface. The inner structures developed from a cylinder to a catenoid and then to a complex structure of catenoid with cylinder. Specifically, the triblock terpolymer has been found to form a long-range ordered perforated lamella in the film. We believe that it is possible to experimentally fabricate a long-range ordered cylindrical catenoid using triblock terpolymer self-assembly under a cylindrical nanopore confinement.

Acknowledgment. We are grateful for the financial support provided by the Outstanding Youth Fund (No. 20525416), the Programs of the National Natural Science Foundation of China (Nos. 20490220 and 90403022), and the National Basic Research Program of China (No. 2005CB623800).

References and Notes

(1) Bates, F. S.; Fredrickson, G. H. *Phys. Today* **1999**, *52*, 32.
(2) Hamley, I. W. *Nanotechnology* **2003**, *14*, R39.
(3) Pereira, G. G. *Curr. Appl. Phys.* **2004**, *4*, 255.
(4) Huinink, H. P.; Brokken-Zijp, J. C. M.; van Dijk, M. A.; Sevink, G. J. A. *J. Chem. Phys.* **2000**, *112*, 2452.
(5) He, X. H.; Song, M.; Liang, H. J.; Pan, C. Y. *J. Chem. Phys.* **2001**, *114*, 10510.
(6) Krausch, G.; Magerle, R. *Adv. Mater.* **2002**, *14*, 1579.
(7) Fraaije, J. G. E. M.; Sevink, G. J. A. *Macromolecules* **2003**, *36*, 7891.
(8) Shin, K.; Xiang, H. Q.; Moon, S. I.; Kim, T.; McCarthy, T. J.; Russell, T. P. *Science* **2004**, *306*, 76.
(9) Arsenault, A. C.; Rider, D. A.; Tetreault, N.; Chen, J. I. L.; Coombs, N.; Ozin, G. A.; Manners, I. *J. Am. Chem. Soc.* **2005**, *127*, 9954.
(10) Sun, Y. M.; Steinhart, M.; Zschech, D.; Adhikari, R.; Michler, G. H.; Gosele, U. *Macromol. Rapid Commun.* **2005**, *26*, 369.
(11) Xiang, H.; Shin, K.; Kim, T.; Moon, S.; McCarthy, T. J.; Russell, T. P. *J. Polym. Sci., Part B: Polym. Phys.* **2005**, *43*, 3377.
(12) Chen, P.; He, X. H.; Liang, H. J. *J. Chem. Phys.* **2006**, *124*, 104906.
(13) Cheng, J. Y.; Ross, C. A.; Smith, H. I.; Thomas, E. L. *Adv. Mater.* **2006**, *18*, 2505.
(14) Feng, J.; Ruckenstein, E. *Macromolecules* **2006**, *39*, 4899.
(15) Yin, Y. H.; Sun, P. C.; Jiang, R.; Li, B. H.; Chen, T. H.; Jin, Q. H.; Ding, D. T.; Shi, C. *J. Chem. Phys.* **2006**, *124*, 184708.
(16) Li, W. H.; Wickham, R. A.; Garbary, R. A. *Macromolecules* **2006**, *39*, 806.
(17) Huinink, H. P.; van Dijk, M. A.; Brokken-Zijp, J. C. M.; Sevink, G. J. A. *Macromolecules* **2001**, *34*, 5325.
(18) Wang, Q.; Nealey, P. F.; de Pablo, J. J. *Macromolecules* **2001**, *34*, 3458.
(19) Knoll, A.; Horvat, A.; Lyakhova, K. S.; Krausch, G.; Sevink, G. J. A.; Zvelindovsky, A. V.; Magerle, R. *Phys. Rev. Lett.* **2002**, *89*, 035501.
(20) Ludwigs, S.; Boker, A.; Voronov, A.; Rehse, N.; Magerle, R.; Krausch, G. *Nat. Mater.* **2003**, *2*, 744.
(21) Wu, Y. Y.; Cheng, G. S.; Katsov, K.; Sides, S. W.; Wang, J. F.; Tang, J.; Fredrickson, G. H.; Moskovits, M.; Stucky, G. D. *Nat. Mater.* **2004**, *3*, 816.
(22) Xiang, H.; Shin, K.; Kim, T.; Moon, S. I.; McCarthy, T. J.; Russell, T. P. *Macromolecules* **2005**, *38*, 1055.
(23) Chen, P.; Liang, H. *J. Phys. Chem. B* **2006**, *110*, 18212.
(24) Park, I.; Park, S.; Park, H. W.; Chang, T.; Yang, H. C.; Ryu, C. Y. *Macromolecules* **2006**, *39*, 315.
(25) Tsarkova, L.; Knoll, A.; Krausch, G.; Magerle, R. *Macromolecules* **2006**, *39*, 3608.
(26) Yu, B.; Sun, P. C.; Chen, T. C.; Jin, Q. H.; Ding, D. T.; Li, B. H.; Shi, A. C. *Phys. Rev. Lett.* **2006**, *96*, 138306.
(27) Li, W.; Wickham, R. A. *Macromolecules* **2006**, *39*, 8492.
(28) Ludwigs, S.; Schmidt, K.; Stafford, C. M.; Amis, E. J.; Fasolka, M. J.; Karim, A.; Magerle, R.; Krausch, G. *Macromolecules* **2005**, *38*, 1850.
(29) Ludwigs, S.; Krausch, G.; Magerle, R.; Zvelindovsky, A. V.; Sevink, G. J. A. *Macromolecules* **2005**, *38*, 1859.
(30) Feng, J.; Ruckenstein, E. *J. Chem. Phys.* **2007**, *126*, 124902.
(31) Sun, P. C.; Yin, Y. H.; Li, B. H.; Chen, T. H.; Jin, Q. H.; Ding, D. T.; Shi, A. C. *J. Chem. Phys.* **2005**, *122*, 204905.
(32) Sun, P. C.; Yin, Y. H.; Li, B. H.; Chen, T. H.; Jin, Q. H.; Ding, D. T.; Shi, A. C. *Phys. Rev. E* **2005**, *72*, 061408.
(33) Yu, B.; Li, B. H.; Sun, P. C.; Chen, T. H.; Jin, Q. H.; Ding, D. T.; Shi, A. C. *J. Chem. Phys.* **2005**, *123*, 234902.